Bilayered V_2O_5 Nanostrands with PVA-Based Cathode Slurry for High-Performance and Sustainable Zinc-Ion Batteries

Kudachchige Asanga G. de Alwis[1,2]*, Zhenhuan Chen[1,2], Dasun P. W. Guruge[1,2], Chathushka D. Hettige Dharmasiri[1,2], Chao Zhang[2,3], Joseph F. S. Fernando[1,2,4], Konstantin L. Firestein[2,3]*, Dmitri V. Golberg[1,2]*

[1]School of Chemistry and Physics, Queensland University of Technology (QUT), 2 George St, Brisbane, Queensland 4000, Australia.

[2]Centre for Materials Science, Queensland University of Technology (QUT), 2 George St, Brisbane, Queensland 4000, Australia.

[3]Central Analytical Research Facility (CARF), Queensland University of Technology (QUT), 2 George St, Brisbane, Queensland 4000, Australia.

[4]Centre for Microscopy and Microanalysis, The University of Queensland, St. Lucia, Queensland 4072, Australia.

Keywords: Zn-ion batteries, Layered V_2O_5, Enhanced ion diffusion, PVA-based binder, Scalable synthesis, high energy density.

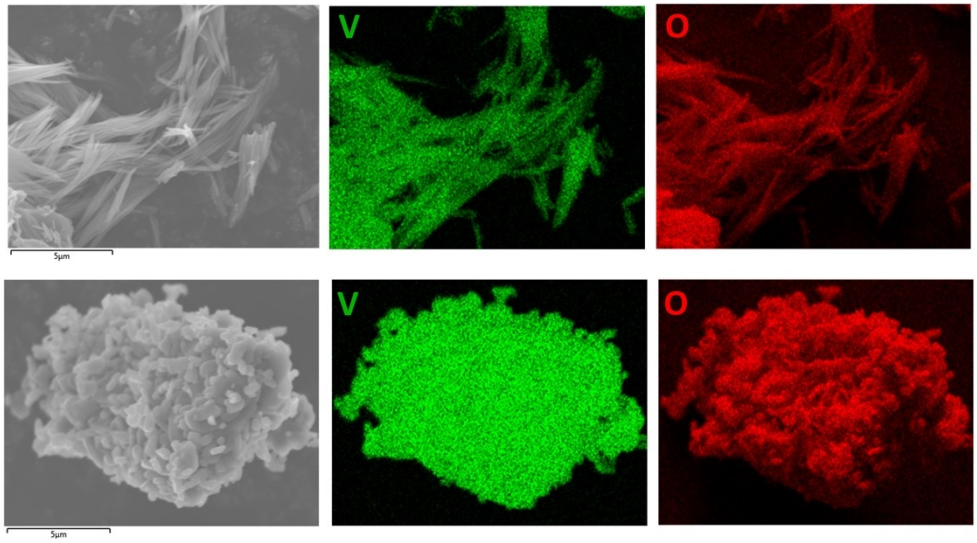

Figure S1. SEM-EDS elemental maps for NS-V_2O_5 (top) and CM-V_2O_5(bottom)indicating the distribution of vanadium (green) and oxygen (red).

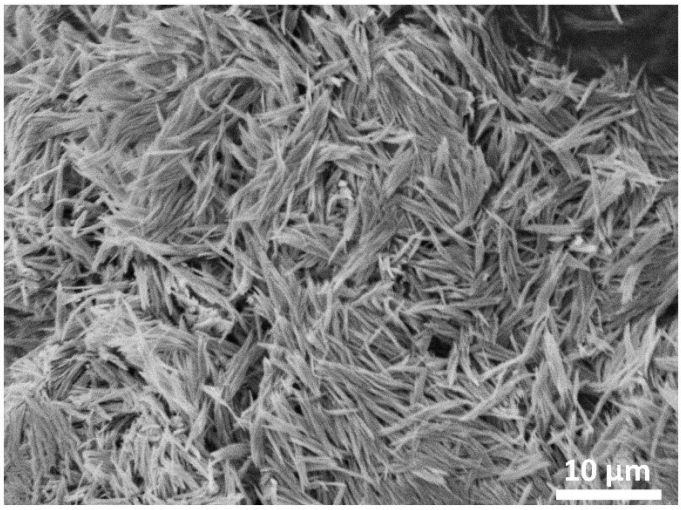

Figure S2. SEM image of NS-PVA-50, obtained via 50-fold scale up process.

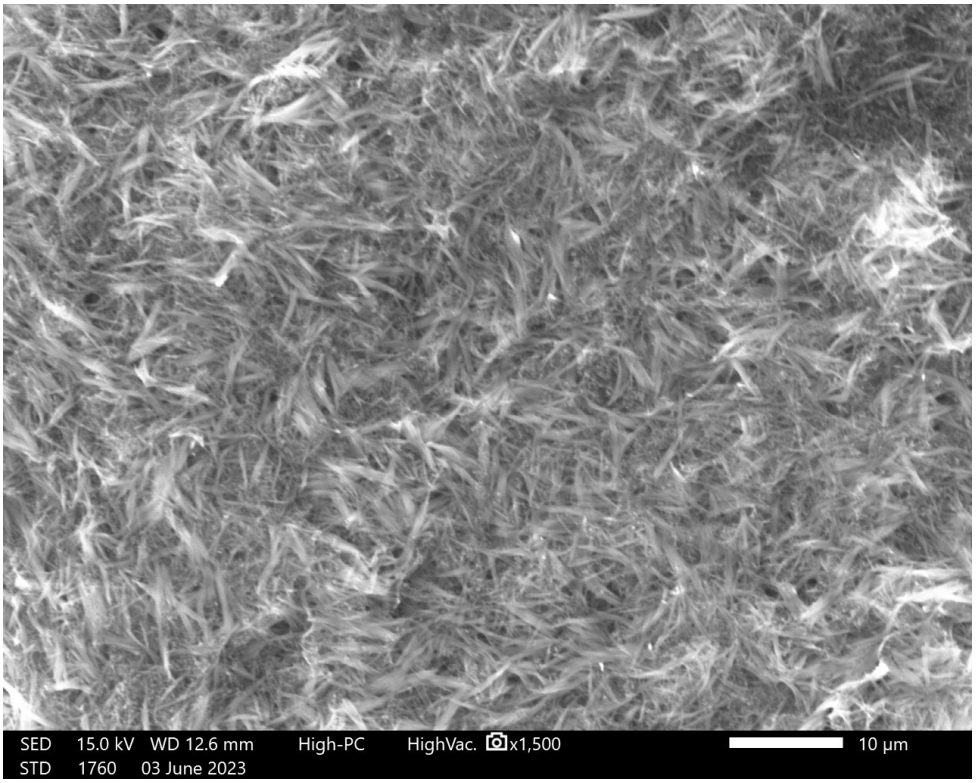

Figure S3. SEM image of NS-PVA slurry coated on to carbon fibre cloth (low magnification).

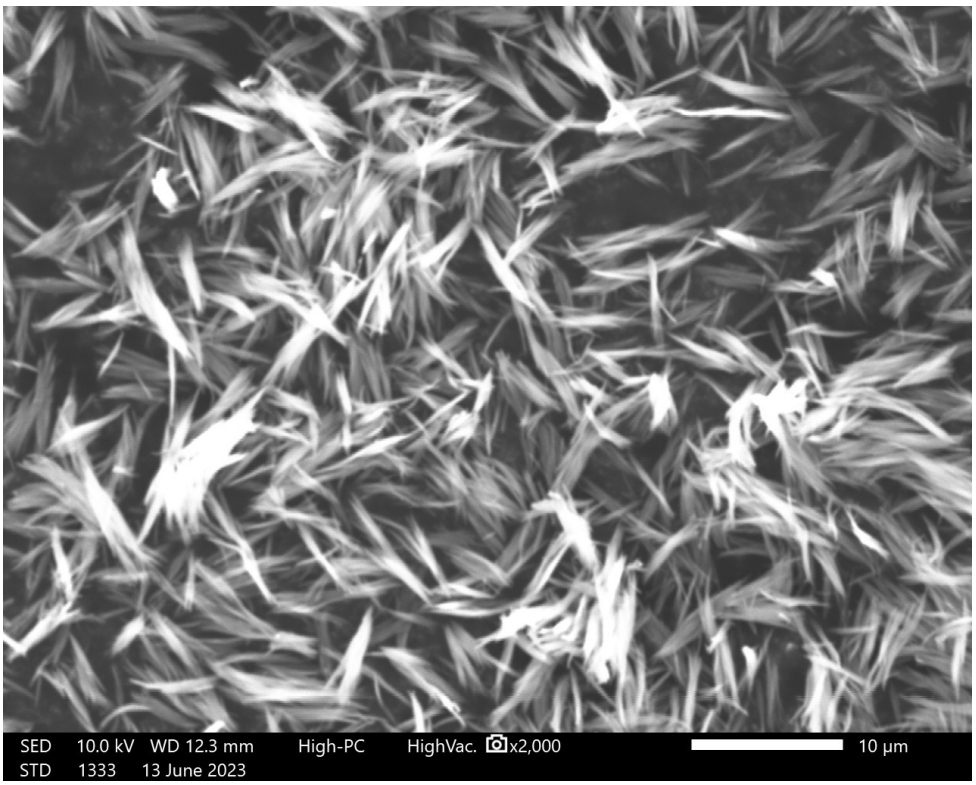

Figure S4. SEM image of NS-PVA slurry coated on to carbon fibre cloth (high magnification).

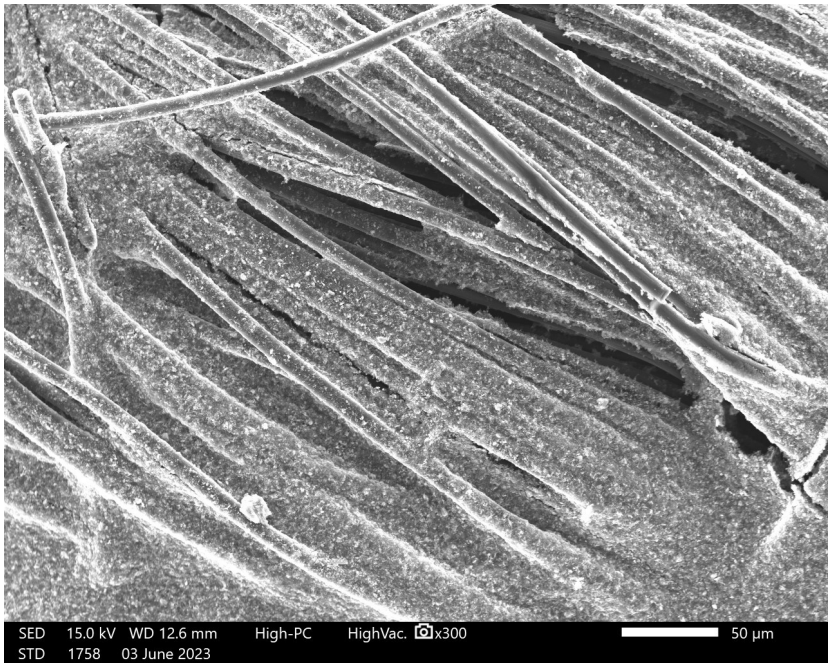

Figure S5. SEM image of CM-PVDF slurry coated on to carbon fibre cloth (low magnification).

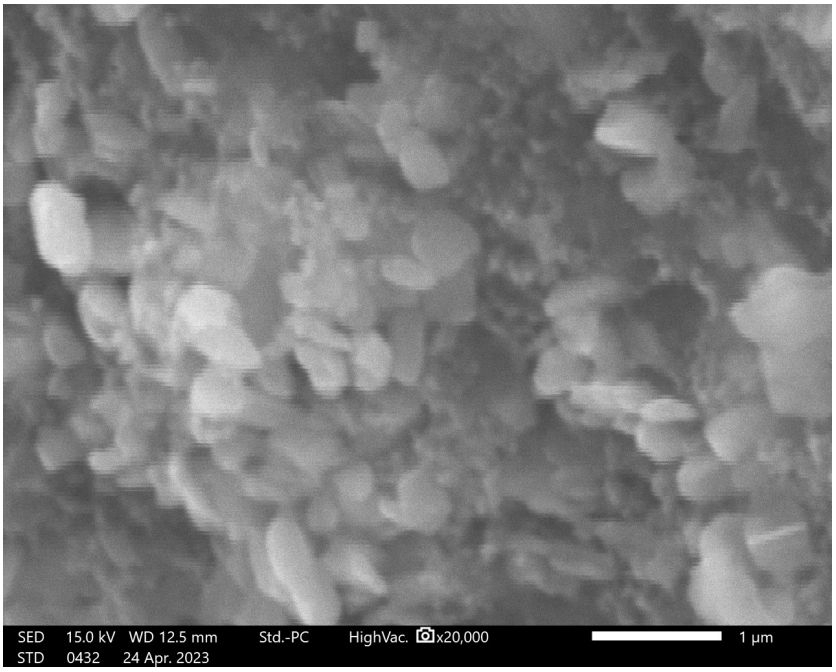

Figure S6. SEM image of CM-PVDF slurry coated on to carbon fibre cloth (high magnification).

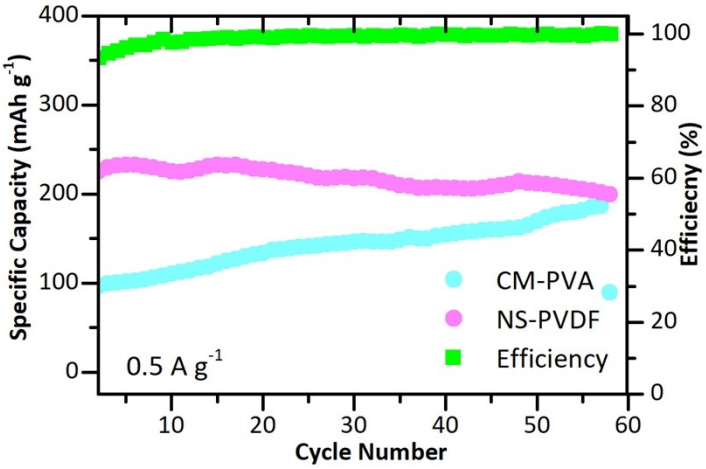

Figure S7. GCD performance at 0.5 A g^{-1} for NS-PVDF and CM-PVA.

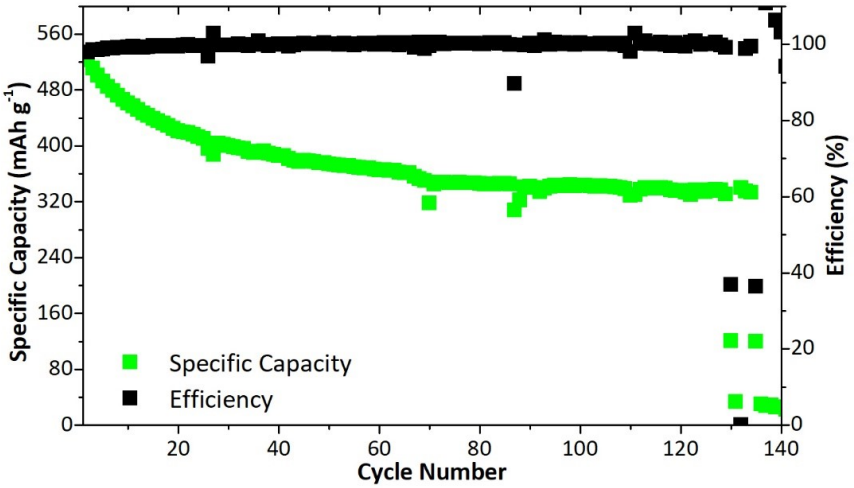

Figure S8. GCD of ZnIINS-PVA-50 – under 0.5 A g^{-1}

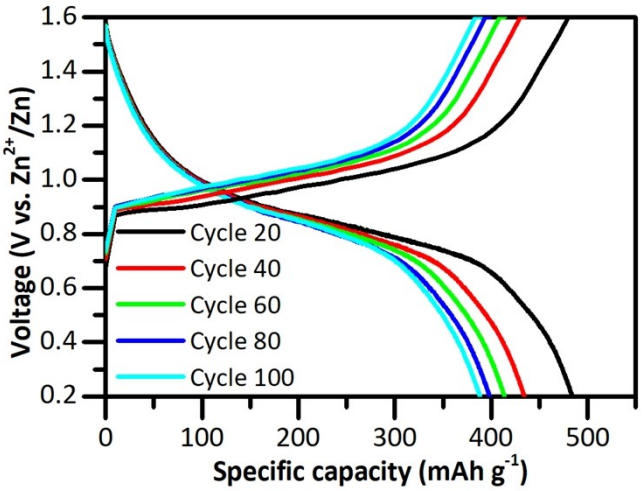

Figure S9. GCD profiles showcasing specific capacity and voltage of NS-PVA full cell at 0.5 A g^{-1}.

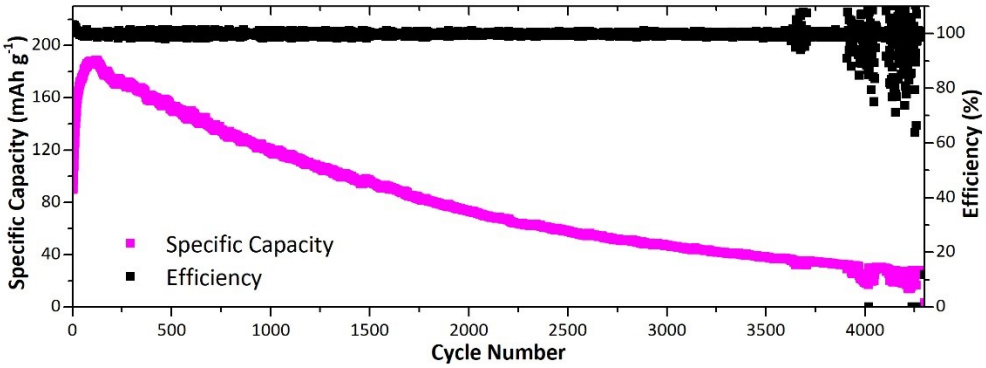

Figure S10. Long-term GCD at 4 A g^{-1} for CM-PVDF with specific capacity and Coulombic efficiency on y-axes.

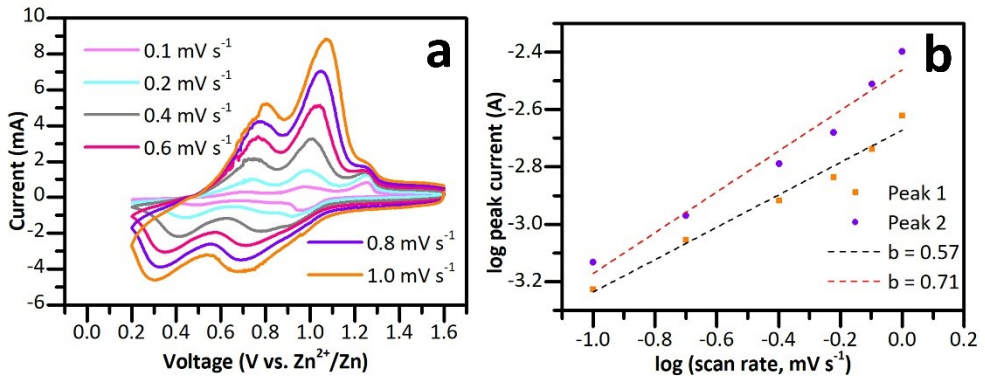

Figure S11. (a) CV curves of CM-PVDF collected at various scan rates ranging from 0.1 to 1.0 mV s^{-1} (b) Log–log plots of peak current versus scan rate for anodic redox peaks.

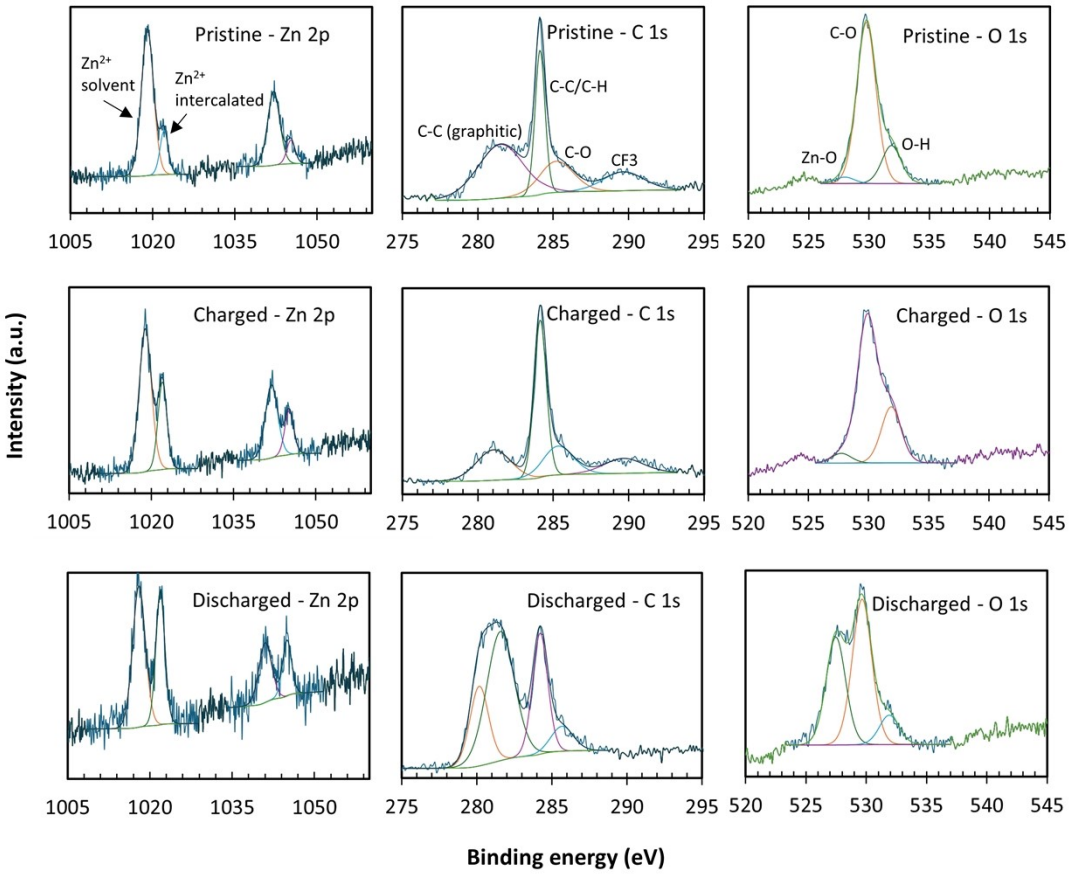

Figure S12. XPS data for pristine, charged and discharged NS-PVA for O 1s, C 1s, and Zn 2p.

Region	Component	Relative abundance (%)		
		Pristine	Charged	Discharged
Zn $2p_{1/2}$	Zn^{2+} (solvent)	27.54	23.34	17.80
	Zn^{2+} (intercalated)	6.04	10.28	11.68
Zn $2p_{3/2}$	Zn^{2+} (solvent)	55.22	45.98	42.37
	Zn^{2+} (intercalated)	11.20	20.40	28.15
O 1s	Zn-O	78.36	68.85	51.43
	C-O	18.45	26.47	38.17
	O-H	3.19	4.67	10.40
C 1s	C-C (graphitic)	18.87	23.8	19.99
	C-C/C-H	24.93	43.44	47.81
	C-O	13.37	19.51	7.44
	CF3	43.13	13.24	24.76

Table S1 Relative abundance (%) for deconvoluted components for O 1s, C 1s, and Zn 2p.

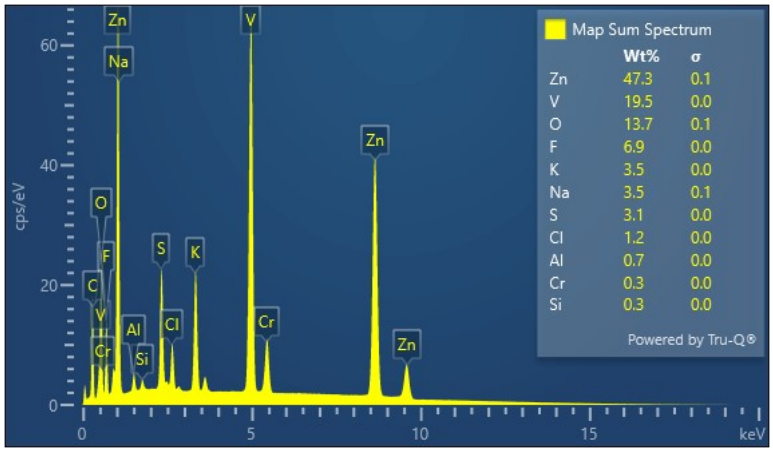

Figure S13. EDS quantitative elemental composition of pristine cathode.

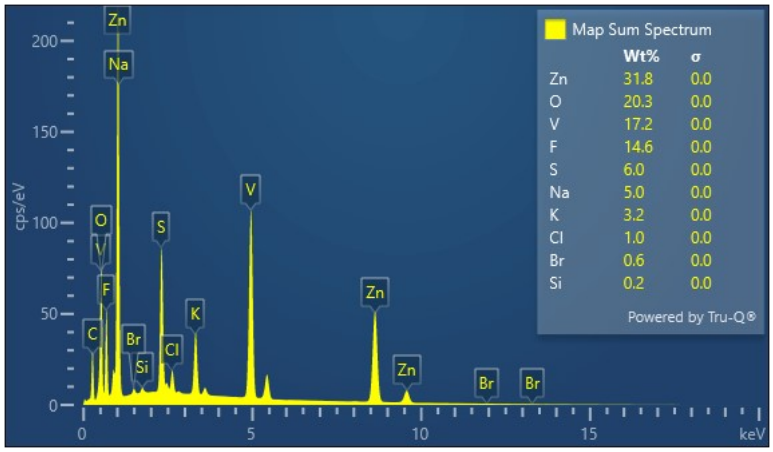

Figure S14. EDS quantitative elemental composition of charged cathode.

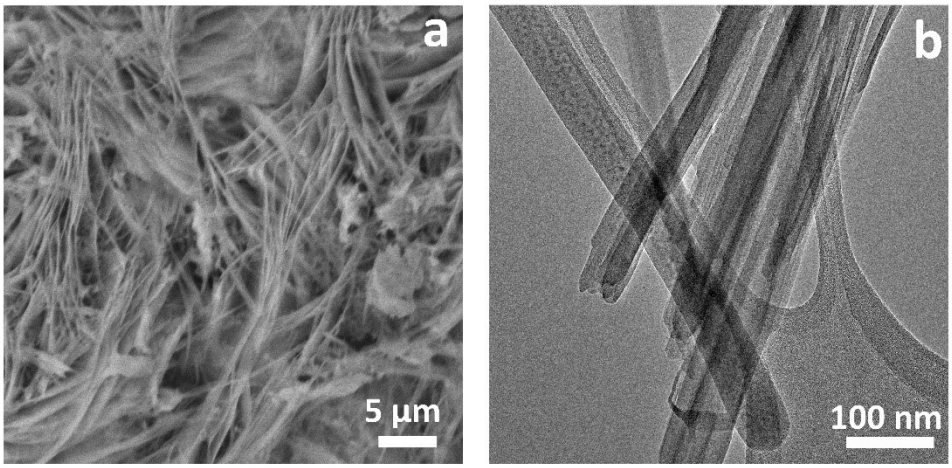

Figure S15. (a) SEM and (b) TEM images of cycled (2000 cycles at 4 A g^{-1}) NS-PVA.

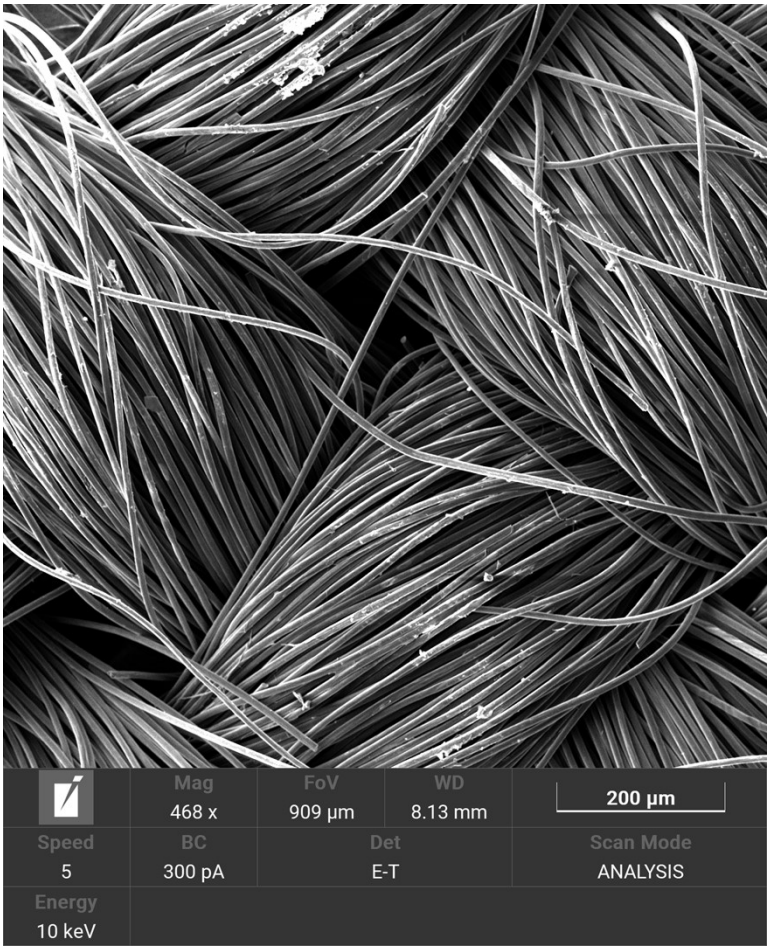

Figure S16. SEM image of the pristine carbon cloth.

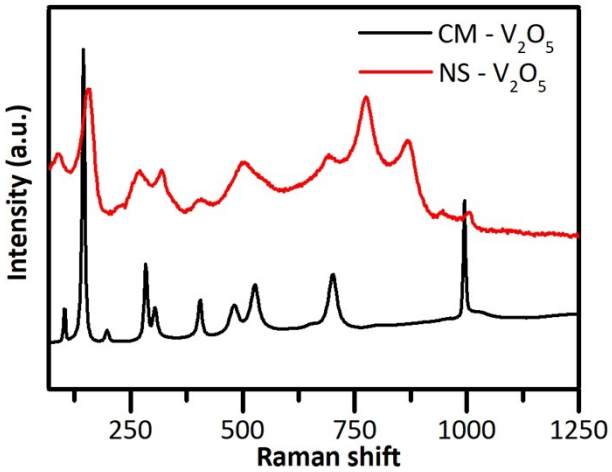

Figure S17. Raman spectra of CM- V_2O_5 and NS-V_2O_5.

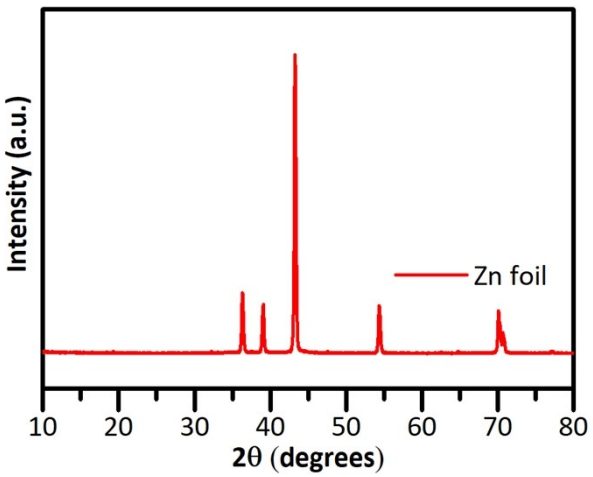

Figure S18. XRD pattern for zinc for used for anode.